Published in final edited form as:
J Invest Dermatol. 2009 July ; 129(7): 1719–1729. doi:10.1038/jid.2008.442.

pH-Regulated Mechanisms Account for Pigment-Type Differences in Epidermal Barrier Function

Roshan Gunathilake[1,5], **Nanna Y. Schurer**[3], **Brenda A. Shoo**[1], **Anna Celli**[1], **Jean-Pierre Hachem**[4], **Debra Crumrine**[1], **Ganga Sirimanna**[5], **Kenneth R. Feingold**[2], **Theodora M. Mauro**[1], and **Peter M. Elias**[1]

1 *Department of Dermatology, Veteran Affairs Medical Center, University of California San Francisco, San Francisco, California, USA*

2 *Department of Metabolism, Veteran Affairs Medical Center, University of California San Francisco, San Francisco, California, USA*

3 *Department of Dermatology, University of Osnabrück, Osnabrück, Germany*

4 *Department of Dermatology, Universitair Ziekenhuis Brussels, Vrij Universiteit Brussel, Brussels, Belgium*

5 *Department of Dermatology, National Hospital of Sri Lanka, Colombo, Sri Lanka*

Abstract

To determine whether pigment type determines differences in epidermal function, we studied stratum corneum (SC) pH, permeability barrier homeostasis, and SC integrity in three geographically disparate populations with pigment type I–II *versus* IV–V skin (Fitzpatrick I–VI scale). Type IV–V subjects showed: (i) lower surface pH (≈0.5 U); (ii) enhanced SC integrity (transepidermal water loss change with sequential tape strippings); and (iii) more rapid barrier recovery than type I–II subjects. Enhanced barrier function could be ascribed to increased epidermal lipid content, increased lamellar body production, and reduced acidity, leading to enhanced lipid processing. Compromised SC integrity in type I–II subjects could be ascribed to increased serine protease activity, resulting in accelerated desmoglein-1 (DSG-1)/corneodesmosome degradation. In contrast, DSG-1-positive CDs persisted in type IV–V subjects, but due to enhanced cathepsin-D activity, SC thickness did not increase. Adjustment of pH of type I–II SC to type IV–V levels improved epidermal function. Finally, dendrites from type IV–V melanocytes were more acidic than those from type I–II subjects, and they transfer more melanosomes to the SC, suggesting that melanosome secretion could contribute to the more acidic pH of type IV–V skin. These studies show marked pigment-type differences in epidermal structure and function that are pH driven.

INTRODUCTION

Survival in a terrestrial environment requires multiple defensive barrier functions, largely provided by the stratum corneum (SC), that protect the living organism against both excessive water loss and relentless insults from the external milieu (Elias, 2005). The epidermal permeability barrier localizes to the SC extracellular matrix, where a mixture of precursor lipids is “processed” into nonpolar species that form broad, hydrophobic lamellar membranes (Elias and Menon, 1991). Maintenance of SC integrity reflects a dynamic balance between

Correspondence: Dr Roshan Gunathilake, Department of Dermatology, Veteran Affairs Medical Center, University of California San Francisco, 4150 Clement Street, San Francisco, California, 94121, USA. E-mail: E-mail: gunathilake@att.net.

CONFLICT OF INTEREST

The authors state no conflict of interest.

intercellular cohesion maintained by unique intercellular junctions, that is, corneodesmosomes (CDs), followed by distal desquamation, a process regulated by protease/antiprotease balance (Caubet *et al*., 2004, Brattsand *et al*., 2005).

The SC has a highly acidic, surface pH ("acid mantle") (Schade, 1928), which was long thought to serve an antimicrobial function (Marchionini and Hausknecht, 1938, Fluhr and Elias, 2002). Yet, SC pH also regulates at least two other critical functions, that is, permeability barrier homeostasis, SC integrity/cohesion (desquamation), and possibly IL-1α/β release from SC (Nylander-Lundqvist *et al*., 1996). Accordingly, permeability barrier recovery is delayed when perturbed skin sites are exposed to a neutral pH buffer (Mauro *et al*., 1998). Similarly, blockade or knockout of either secretory phospholipase A2 activity or the sodium-proton exchanger (sodium-proton exchanger) (both important contributors to SC acidity) compromises both permeability barrier homeostasis and SC integrity/cohesion (Fluhr *et al*., 2001, Behne *et al*., 2002). Finally, elevations of pH in normal skin perturb both permeability barrier homeostasis and SC integrity/cohesion, further linked to increased activity of serine proteases (SPs), key enzymes of normal desquamation (Hachem *et al*., 2003, 2005), and reduced activities of two ceramide-generating enzymes with acid pH optima, that is, β-glucocerebrosidase and acidic sphingomyelinase.

There is a paucity of information about differences in epidermal function among human populations of divergent pigment types. Most of the earlier studies instead have examined "racial" or "ethnic," rather than pigment-type-dependent differences in barrier function, with conflicting or inconclusive results due to either small sample size or large intersubject variations (reviewed by Rawlings, 2006). Moreover, genetic linkage studies indicate that there is no true racial profile—only variations in degrees of pigment (McEvoy *et al*., 2006). In a small preliminary study, we showed previously that pigment type (not ethnicity) seemed to determine differences in barrier function and SC cohesion (Reed *et al*., 1995). To establish definitively whether pigment type determines differences in epidermal barrier function among normal subjects of divergent pigment types, we assessed here epidermal function in three geographically disparate populations with either pigment type I–II or IV–V skin (Fitzpatrick, 1988). Our results show that subjects with darkly pigmented skin show enhanced epidermal function, and that differences in epidermal lipid content and pH-regulated enzymatic mechanisms account for these variations. Conversely, we show that acidification of type I–II SC with topical polyhydroxyl acids equalizes epidermal function in these disparate pigment types. Finally, we demonstrate that vesicular organelles that correspond to melanosomes in dendritic processes in darkly pigmented melanocytes are significantly more acidic and persist high into the epidermis, providing a cellular mechanism whereby melanocytes could acidify the SC of darkly pigmented subjects.

RESULTS

Type IV–V subjects show enhanced epidermal function

We first compared epidermal permeability barrier homeostasis and SC integrity/cohesion in two cohorts of subjects with divergent pigment types, studied during the summer months of 2006 (Table 1). As in our previous study (Reed *et al*., 1995), the darkly pigmented (type IV–V) Sri Lankan cohort displayed faster barrier recovery, assessed as the kinetics of recovery 24–72 hours after acute barrier abrogation, in comparison with the lightly pigmented German cohort, with Fitzpatrick type I–II skin (Figure 1a). This finding was somewhat unexpected, as prolonged exposure to a high relative humidity delays barrier recovery in experimental animals (Denda *et al*., 1998). Furthermore, these type IV subjects also showed significantly enhanced SC integrity (51.7 ± 5.4 *vs* 20.1 ± 0.5 tape strippings required to increase transepidermal water loss (TEWL) threefold in type IV–V *vs* I–II subjects; $P < 0.0001$), and increased SC cohesion

(4.36 ± 0.89 *vs* 9.19 ± 1.53 μg of protein removed per tape strip; $P < 0.05$) (Figures 1b and c). The baseline TEWL for the two populations was normal, that is, ≤ 10 gm^{-2} $hour^{-1}$.

As local differences in temperature, relative humidity, and/or UV exposure in these two, widely separated geographical locations could impose potentially confounding variables, we next assessed epidermal functions in a group of age- and gender-matched subjects of divergent pigment types living in the same geographical location (San Francisco, CA). In this group of subjects, functional end points were compared at an earlier time point, that is, 3 hours after barrier recovery, when the maximum divergence of function occurred. As with the geographically divergent cohorts, the darkly pigmented subjects again showed enhanced permeability barrier function and SC integrity (Figure 2). Pertinently, the absolute rates of recovery were faster in darkly pigmented subjects in San Francisco, presumably because of lower ambient relative humidities (op. cit.). Together, these results show that disparities in geographical location cannot account for pigment type-determined differences in epidermal function.

The lower pH of SC correlates with enhanced function in darkly pigmented skin

As both epidermal permeability barrier function and SC integrity/cohesion are regulated by changes in SC pH (Hachem *et al*., 2003, 2005, 2006), we next assessed SC pH in type IV–V *versus* I–II subjects. The darkly pigmented subjects showed a significantly more acidic surface pH than lightly pigmented subjects over two different body surfaces (volar forearm pH 4.6 ± 0.03 *vs* 5.0 ± 0.04, $P < 0.0001$) (Figure 3). These differences in surface pH were independent of gender or occupation (both cohorts were primarily female nursing personnel, aged 20–40 years) (Table 1). Moreover, latitude-dependent differences were not responsible, as similar pH values were found in both the darkly *versus* lightly pigmented San Francisco cohort (c.f. Figure 2). Thus, pigment-type-dependent differences in epidermal function correlate with differences in SC acidification.

Increased epidermal lipid content and lamellar body density in darkly pigmented subjects

To identify mechanism(s) that could account for pigment-type-dependent differences in barrier function, we next assessed epidermal lipid content and lamellar body (LB) secretion in type I–II *versus* IV–V subjects (all samples were from the San Francisco cohort). Subjects with type IV–V skin showed a visible increase in the density of LB in the stratum granulosum in comparison with type I–II epidermis (Figures 4a and b), a finding that was confirmed quantitatively (Figure 4c). Increased LB production correlated with a readily apparent increase in epidermal lipid content, shown in frozen sections stained with Nile Red (Figures 4d and e). Yet, there were no observable differences in the quality or quantities of lamellar bilayer structure between the two pigment groups (not shown). These results suggest that increased epidermal lipid production, leading to increased LB numbers and secretion, could contribute to enhanced barrier function of darkly pigmented skin.

Increased corneocyte envelope thickness in type IV–V subjects

The corneocyte, by providing a necessary scaffold for extracellular bilayer organization, contributes to permeability barrier function (Elias *et al*., 2002). Whereas we detected no differences in the corneocyte cytosol, darkly pigmented subjects showed a significantly thicker cornified envelopes (CEs) in comparison with lightly pigmented subjects (19.7 ± 0.6 *vs* 15.5 ± 0.4nm for type IV–V and I–II subjects, respectively; $P < 0.0006$) (Figure S1a). Yet, despite showing thicker CE, we found no visible differences in immunostaining for several constituent CE peptides, including loricrin, filaggrin, and involucrin, in darkly *versus* lightly pigmented epidermis (Figure S1b). Thus, although darkly pigmented SC displays a thicker CE, the basis for this difference remains unknown.

Basis for pigment-type differences in SC integrity and cohesion

We next examined mechanisms that could explain pigment-type differences in SC integrity/cohesion. Although a greater number of cell layers could account for the larger number of tape strippings needed to abrogate the barrier, our results show no significant difference in either the number of SC cell layers or SC thickness in the two pigment types (19.6 ± 3.6 *vs* 17.1 ± 1.7 cell layers for type I–II and IV–V subjects, respectively; NS). We next assessed the basis for enhanced cohesion of darkly pigmented SC. Although CDs were progressively degraded in the lower SC layers of subjects with type I–II skin, disappearing in the mid-to-outer SC, they persisted to much higher levels of SC in type IV–V subjects (Figure 5a and b). These ultrastructural observations were confirmed by quantitative studies (Figure 5c). Finally, we assessed desmoglein-1 (DSG-1) distribution and persistence in darkly *versus* lightly pigmented SC by immunofluorescence. In agreement with the electron microscope studies on CD density, DSG-1 appeared to be retained high into the outer SC of darkly pigmented subjects, whereas DSG-1 immunostaining was restricted to the lower SC in lightly pigmented subjects (Figure 5d). These results show differences in CD structure and content that correlate with pigment type.

Enzymatic basis for differences in SC integrity and cohesion

We next assessed whether the enhanced SC integrity/cohesion and CD retention of type IV–V skin could be attributed to reduced SP activity. Using *in situ* zymography, type IV–V SC, with its more acidic pH, showed lower SP activity compared with lightly pigmented skin (Figure 6a). As SP activity returned to comparable levels in the two groups after *in situ* neutralization (Figure 6a, insets), the observed differences in the activity are most likely to be pH driven, rather than being attributable to different levels of enzyme protein.

Yet, even with CD persistence, type IV–V SC does not show an increased number of cell layers (see above). As cysteine and aspartate proteases, two protease families with acidic, rather than neutral, pH optima, also regulate desquamation (Horikoshi *et al*., 1999; Caubet *et al*., 2004), we next assessed whether increased activity of these proteases could account for the maintenance of normal SC thickness in type IV/V subjects. Subjects with skin types IV–V displayed increased cathepsin D activity in the outer SC, whereas little cathepsin D activity could be detected in type I–II SC (Figure 6b). The specificity of these zymographic results was further shown by the blockade of activity by the broad aspartate protease inhibitor, pepstatin (not shown).

Acidification of SC optimizes epidermal functions in type I–II subjects

To further test whether the diminished function of type I–II skin results from a higher SC pH, we next examined whether downward adjustment of SC pH to levels comparable with type IV–V subjects would improve function in type I–II subjects. We applied two polyhydroxyl acids (that is, lactobionic acid (LBA) or gluconolactone (GL)) to lower pH to levels comparable with type IV–V skin (Figure 7a–c).

To determine whether acidification with topical PHAs (as above) accelerates barrier recovery kinetics in type I–II human skin, we assessed barrier recovery kinetics following acute abrogation, 24 hours after single applications of either LBA or GL. If applied immediately after tape stripping, both LBA and GL significantly accelerated barrier recovery at 1, 6, and 24 hours, in comparison with either vehicle or neutralized LBA/GL (Figure 7d). Thus, acidification by topical application of PHAs enhances permeability barrier function of type I–II SC to levels comparable with type IV–V skin.

Melanocyte cytosol and dendrites of darkly pigmented subjects are more acidic

In preliminary studies, we investigated whether differences in expression/activity of certain endogenous, epidermal acidifying mechanisms, that is, sodium-proton exchanger and SPLA2, could account for pigment-type-dependent differences in epidermal function. As we could not detect differences in these mechanisms (not shown), we next assessed whether differences in melanocyte biology could account for the functional differences. We assessed whether melanocytes show inherent differences in acidification that could contribute to the lower pH of darkly pigmented skin sites. To measure the cytosolic pH of melanocytes derived from lightly pigmented and darkly pigmented human skin, we applied the pH-sensitive, fluorescent probe, seminaphthorhodafluorescein- 5F (SNARF-5F) (Bassnett *et al*., 1990, Whitaker *et al*., 1991, Hunter and Beveridge, 2005), to cultured human melanocytes, followed by life-time, two-channel imaging by confocal microscopy.

We assessed the pH of the cell bodies and dendrites of a total of 27 lightly pigmented melanocytes and 33 darkly pigmented cells (Figure 8a). The mean pH of the cell bodies was 7.2 ± 0.1 and 7.3 ± 0.1 for the darkly *versus* lightly pigmented melanocytes, respectively (Figure 8b, $P < 0.05$).

Dendritic processes, which concentrate and secrete melanosomes, showed a still further decline in pH in darkly *versus* lightly pigmented melanocytes (mean pH 6.9 ± 0.2 *versus* 7.1 ± 0.1; $P < 0.001$) (Figure 8b), and acidity further localized to vesicular organelles that most likely represent melanosomes (Figure 8a). These results show that melanocytes, and particularly the dendrites, from darkly pigmented subjects are significantly more acidic than those from lightly pigmented subjects, and that this acidity appears to localize to melanosomes.

Finally, we prepared organotypic cocultures of type II and type V human melanocytes, with keratinocytes from un-related type II humans, and compared transfer and persistence of melanosomes in the resulting epidermal equivalents. As seen both by electron microscope and Fontana Masson staining, many more melanosomes are retained into the outer epidermis and SC of cocultures with type V melanocytes (Figure S2a–e). Taken together, these results provide a cellular mechanism whereby the pH of SC could be further reduced in darkly pigmented epidermis.

DISCUSSION

Previous studies of divergent pigment types in humans have yielded inconsistent differences in barrier function, perhaps because they assessed ethnic groups, such as Caucasians and African-Americans, rather than pigment-type-determined differences (Berardesca *et al*., 1998). In our preliminary study, an increase in pigment appeared to correlate with superior barrier properties, independent of ethnicity (Reed *et al*., 1995). The present study confirms that there are significant functional differences between subjects with type I–II *versus* type IV–V skin. Subjects with skin types IV–V showed superior SC integrity, independent of ethnicity, gender, and age, that is, ≈2.5 × more tape strips were required to produce levels of barrier abrogation comparable with skin types I–II. Moreover, the darkly pigmented subjects also showed superior permeability function, observed as significantly faster barrier recovery rates after acute barrier disruption. Again, superior barrier function in pigmented skin is independent of ethnicity, age, gender, season, and latitude, that is, the differences were readily discernible in three geographically distinct, age-, gender-, and even occupation-matched groups of subjects (both the German and Sri Lankan cohorts were primarily nursing personnel).

Prolonged exposure to a reduced relative humidity enhances barrier function, whereas conversely, exposure to an elevated relative humidity downregulates it (Denda *et al*., 1998). Hence, it could be argued that the differences in epidermal function observed in subjects living

in Germany *versus* Sri Lanka could have resulted from adaptation to different climatic conditions. Seasonal differences have also been shown to influence epidermal ceramide levels (Rogers *et al*., 1996), which could further accentuate functional differences. However, our data from the third cohort of subjects with divergent pigment types, living in San Francisco, show that this is not the case. Taken together, these epidermal functional differences could account for differences in the severity of a number of skin disorders that are accompanied or driven by a barrier abnormality. For example, fair-skinned individuals exhibit an increased propensity to develop cutaneous infections and eczematous dermatoses (Mackintosh, 2001). Accordingly, a higher surface pH is well known to favor growth of common microbial pathogens, and to inhibit the growth of normal flora (Korting *et al*., 1990).

We also assessed here certain mechanisms that could account for the pigment-type-determined differences in function. Surface pH is significantly lower in type IV–V than in type I–II skin, and pH regulates both SC integrity/cohesion, as well as permeability barrier homeostasis (Hachem *et al*., 2003, 2005, Fluhr *et al*., 2004). We therefore hypothesized that downstream, pH-regulated mechanisms could underlie these functional differences. The type IV–V epidermis showed enhanced lipid production and LB density in comparison with type I–II epidermis, although lamellar bilayer morphology appeared similar in both groups. Although it is most likely that the increased number of preformed LB that cluster at the stratum granulosum (SG)–SC interface are transformed more rapidly into mature lamellar bilayers, we were unable to quantitate differences in bilayer morphology between the two pigment groups.

Although the lower pH of darkly pigmented SC could increase the activities of the two key lipid-processing enzymes with acidic pH optima, β-glucocerebrosidase and acidic sphingomyelinase (Hachem *et al*., 2003, 2005), we could not detect differences in their activity by *in situ* zymography, most likely due to the low sensitivity of this assay over this pH range. As we also could not find ultrastructural evidence for increased lamellar bilayers in darkly pigmented skin, enhanced barrier function in type IV–V skin most likely reflects (1) additional bulk lipid at the SC–SG interface; (2) subtle differences in lipid processing; and/or (3) improved SC integrity/cohesion, which also contributes to barrier function (Cork *et al*., 2006). Under basal conditions, it is also possible that much of the excess lipid is absorbed and reutilized by various salvage pathways (Uchida and Holleran, 2008).

The SC SPs, kallikrein 5 (SC tryptic enzyme) and kallikrein 7 (SC chymotryptic enzyme), show neutral pH optima, and both are convincingly linked to desquamation (Brattsand and Egelrud, 1999; Ekholm *et al*., 2000). Accordingly, the more acidic pH of darkly pigmented skin appeared to reduce SP activity, whereas conversely, the neutral pH of lightly pigmented SC instead appeared to increase SP catalytic activity, as shown here by *in situ* zymography. Our results further show that these pH-related alterations in SP activity are associated with different rates of CD/DSG-1 degradation in the two pigment groups. Thus, the pigment-type differences in SC integrity and cohesion can most likely be attributed to different rates of SP-mediated degradation of CD.

Interestingly, the number of SC cell layers did not increase in darkly pigmented SC, despite low SP activity and persistence of CD into the mid-to-outer SC. We showed here that the aspartate protease, cathepsin D, is activated in the outer SC of darkly pigmented subjects, most likely restricting SC thickness. Furthermore, as cathepsin D activates transglutaminase- 1 (Egberts *et al*., 2004), increased transglutaminase-1 activity could explain the thicker CE in the darkly pigmented subjects, a structural change that could correlate with enhanced scaffold function (as well as superior mechanical resistance) in darkly pigmented skin. Yet, the other class of proteases, with acidic pH optima, cysteine proteases, reportedly show a quite different, if not opposing, pattern to pigment-type-dependent expression (Chen *et al*., 2006). Finally, as a direct test of this pH-driven hypothesis, we showed that the adverse consequences of an

elevated SC pH in lightly pigmented subjects could be reversed by lowering SC pH to levels comparable with darkly pigmented subjects. Whereas we used PHAs to lower pH, others have shown that α-hydroxyacids also improve barrier function in parallel with a reduction in pH (Rawlings *et al*., 1996, Berardesca *et al*., 1997).

Our studies also provided insights into at least one mechanism, whereby melanocytes could influence epidermal function. We found that darkly pigmented melanocytes show a lower pH, and that their dendrites showed vesicular organelles that could correspond to melanosomes. Melanosomes are acidic organelles (Puri *et al*., 2000), and previous workers have shown that their pH is inversely correlated with the degree of melanization (Bhatnagar *et al*., 1993). Furthermore, there appears to be a size gradient of melanosomes, their size increasing from lightly to darkly pigmented skin types (Szabo *et al*., 1969, Jimbow *et al*., 1976, Thong *et al*., 2003). Moreover, darkly pigmented melanocytes distribute more melanosomes to the outer epidermis of neighboring keratinocytes in organotypic cultures, potentially explaining the pH disparity in lightly *versus* darkly pigmented subjects. Thus, the transfer of additional and/or more acidified organelles from the melanocytic dendrites could account, at least in part, for the lower pH of SC in darkly pigmented subjects.

MATERIALS AND METHODS

Human subjects

Written, informed consent was obtained from all participants before enrollment, and all clinical investigations were conducted according to the Declaration of Helsinki principles. The research protocol was approved by the human studies committees at the University of California, San Francisco, Veterans Affairs Medical Center, San Francisco, University of Osnabruck, FRG, and the National Hospital of Colombo, Sri Lanka.

Skin surface pH was measured in 110 healthy nurses (72 females, mean age 29 ± SD 6.6) with type I–II skin (Fitzpatrick scale) working at the University of Osnabruck, Osnabruck, Germany, and in 129 nurses (117 females, mean age 25 ± SD 2.1 years) with type IV–V skin, working at the National Hospital, Colombo, Sri Lanka. Epidermal integrity was assessed in two groups of healthy volunteers, each having 20 subjects with type I–II (age 31.8 ± SD 6.9 years) and type IV–V (age 32.4 ± SD 9.7 years) skin.

To ascertain if the results from the functional studies are reproducible in subjects of pigment extremes from the same geographic location, functional measurements were repeated in 17 healthy volunteers (10 subjects with type I–II and 7 subjects with type IV–V skin pigment types) at the Veteran Affairs Medical Hospital, San Francisco, CA. Normal human skin was obtained for morphological and tissue culture studies from fresh surgically resected “dog ears,” in compliance with Declaration of Helsinki principles.

Functional studies

Volunteers refrained from using skin-cleansing agents or other local applications for at least 48 hours before and during the study. Subjects with current or previous skin disease were excluded. After a 15-minute acclimatization period, functional measurements were taken in a controlled environment with temperature and relative humidity set between 22 and 25 °C and between 40 and 60%, respectively. A flat glass electrode (Mettler-Toledo, Giessen, Germany), attached to a precision pH meter (pH 900; Courage & Khazaka, Cologne, Germany), was used to measure skin surface pH on the volar forearm and the dorsa of the nondominant hands of the volunteers.

To assess SC integrity and permeability barrier recovery, TEWL was first measured under basal conditions, on a circular area of 1 cm diameter, on the volar aspect of the nondominant

forearm, using a Tewameter (TM 300; Courage & Khazaka) following the guidelines (Pinnagoda *et al*., 1990). TEWL values were registered in gm^{-2} $hour^{-1}$ after equilibration of the probe on the skin. Sequentially, 3M Blenderm tape strips (3M Health Care, Neuss, Germany) were pressed, with comparable pressure to the test sites for about 3 seconds each, and removed with forceps. TEWL levels were measured after every five tape strippings. Tape stripping was repeated until TEWL increased by threefold. Barrier recovery was evaluated at 24, 48, and 72 hours after tape stripping. For calculation of the percentage change in TEWL, the following formula was used: (TEWL immediately after stripping−TEWL at the indicated time)/(TEWL immediately after stripping−baseline TEWL) × 100%.

To assess SC cohesion, sequential D-squame tapes were applied on the volar forearm of healthy volunteers as described above, and removed until TEWL is increased by threefold. Amount of protein removed per tape was estimated using Bio-Rad protein assay, as described previously (Dreher *et al*., 1998).

Acidification studies

Sixteen normal human volunteers (four males and twelve females; ages 32 ± 9 years) were included after providing informed consent. To modulate the pH sustainably on the forearms of human volunteers, we applied 500 μl of (1) LBA and NaOH-neutralized LBA (5% vol/vol in propylene glycol/ethanol, 7:3, pH 3.2), (2) GL and NaOH-neutralized GL, or (3) vehicle, without occlusion, randomly to contralateral forearms. Surface pH was measured at 1, 6 and 24 hours after LBA/GL or vehicle application.

To assess permeability barrier function, TEWL was measured first under basal conditions, as well as immediately following acute barrier disruption by repeated D-squame tape stripping (20–25 Dsquame tapes increased EWL to ≥20 $mgcm^{-2}$ $hour^{-1}$), and 3, 24, and 48 hours after application of LBA/neutralized LBA, GL/neutralized GL, and propylene glycol/ethanol vehicle. The area under the curve was calculated.

Ultrastructural and quantitative morphological studies

Biopsy samples were minced to < $0.5mm^3$, fixed in modified Karnovsky's fixative (2% paraformaldehyde, 2% glutaraldehyde, 0.1M cacodylate buffer, pH 7.4) overnight, and postfixed with either 0.25% ruthenium tetroxide or reduced osmium (1% aqueous osmium tetroxide, 1.5% potassium ferrocyanide). After postfixation, samples were dehydrated in a graded ethanol series, and embedded in an Epon-epoxy mixture. Ultrathin sections were cut on an ultramicrotome (Leica Ultracut E, Nussloch, Germany) and examined in an electron microscope (Zeiss 10A; Carl Zeiss, Thornwood, NY) operated at 60 kV. At least 10 random images from each subject (n = 5 from each pigment group) were taken at × 25 by an unbiased observer and used for quantitative assessments.

CD/CE length—The ratio between total length of intact CDs to total length of cornified envelopes was determined in the first two layers above the SC–SG junction, and in the 2–3 outermost layers of the SC by planimetry (n = 5 subjects from each pigment group).

LB density—Lamellar body density was measured in the two SG layers, immediately beneath the SC–SG junction by randomly superimposing a stereological grid and counting "hits" *versus* "non-hits." LB density was expressed as hits/(hits + nonhits) × 100 (n = 5 subjects from each pigment group).

Lamellar bilayers—The quality and quantity of the lamellar bilayers in the SC was assessed in randomized, coded micrographs after ruthenium tetroxide postfixation by a blinded observer (P.M.E.).

Cornified envelope—Changes in CE thickness of corneocytes in the outer and lower SC in each subject were measured in randomized, coded electron micrographs using Gattan software. At least 30 measurements were taken from at least 5 subjects in each pigment group.

SC thickness—The number of cell layers in the SC was counted in at least two low-power (× 3,000) electron micrographs from each subject (n = 5 for each pigment group).

In situ zymographic assays

Serine protease—Surgical biopsies (n = 4 from each pigment group) were snap-frozen and stored at −80 °C. Frozen sections (7 μm) were rinsed with washing solution (0.025% Tween-20 in deionized water) and incubated at 37 °C for 2 hours with 250 μl BODIPY-Fl-casein (1 μg μl^{-1}) in deionized water (3 $\mu l ml^{-1}$). Some sections were exposed to the fluorophore substrate in a neutral buffer (4-(2- hydroxyethyl)-1-piperazineethanesulfonic acid buffer, pH 7.4). Sections were then rinsed with 0.025% Tween-20 washing solution, coverslipped, counterstained with propidium iodide (Sigma Aldrich, Bornem, Belgium), and visualized under a confocal microscope (Leica TCS SP, Heidelberg Germany) at an excitation length of 485nm and emission wavelength of 530 nm. Zymographic assays of enzyme activity, although not quantitative, show *in situ* activity more accurately than *in vitro* assays, where the pH of the buffer solution artificially changes activities (for example, Hachem *et al*., 2003, 2005).

Cathepsin D—Frozen sections (7 μm) were rinsed with washing solution (0.025% Tween-20 in deionized water) and incubated at 37 °C for 2 hours with 250 μl BODIPY-Fl-pepstatin A (1 μg μl^{-1}) in deionized water (1 $\mu l ml^{-1}$). Sections were then rinsed with 0.025% Tween-20 washing solution, coverslipped, counterstained with propidium iodide (Sigma Aldrich), and visualized under a confocal microscope (Leica TCS SP) at an excitation length of 485nm and emission wavelength of 530 nm.

Immunohistochemistry and immunofluorescence

Immunohistochemical staining for assessment of changes in epidermal differentiation was performed as described earlier (Demerjian *et al*., 2006). Briefly, after deparaffinization, 5 μm sections were incubated with the primary antibodies overnight at 4 °C. After washes ×3, sections were incubated with the secondary antibody for 30 minutes. Staining was detected with ABC-peroxidase kit obtained from Vector Labs (Burlingame, CA). After counter-staining with hematoxylin, sections were visualized under a light microscope, and digital images were captured with AxioVision software (Carl Zeiss Vision, Munich, Germany).

Immunofluorescence was used to detect DSG-1. After deparaffinization, 5 μm paraffin sections were rehydrated with distilled water, washed with 1 ×TBS, incubated for 30 minutes in blocking buffer (1% bovine serum albumin, 0.1% cold-water fish gelatin in phosphate buffered saline), and were then incubated overnight at 4 °C with mouse anti-human DSG-1 monoclonal antibody (Millipore, Billerica, MA) in blocking buffer. Tissue sections were then washed with 1 × TBS, and incubated for 1 hour with Alexa Fluor 488 secondary antibody in blocking buffer, counterstained with propidium iodide (Sigma Aldrich), and visualized in a confocal microscope (Leica TCS SP) at an excitation length of 485nm and emission wavelength of 530 nm.

Lipid and melanin detection

Frozen sections (7 μm) were incubated with Nile Red (Sigma Aldrich) in 75% glycerol (2 $\mu g ml^{-1}$) for 5 min and visualized in a confocal microscope (Leica TCS SP) at an excitation length of 485nm and emission wavelength of 530 nm.

Fontana–Masson stain for melanin detection

After deparaffinization, 5 μm sections were incubated with fresh ammoniacal silver solution in a 55 °C water bath for 30 minutes. Slides were then placed in 0.1% gold chloride for 1 minute and in 5% sodium thiosulphate for 2 minutes, counterstained with Nuclear Red fast, and visualized under a light microscope. Digital images were captured with AxioVision software (Carl Zeiss Vision).

Two-channel confocal imaging of cultured keratinocytes

Human melanocytes from darkly and lightly pigmented neonatal foreskin samples ($n > 3$ each) were plated in separate four-well coverslips in a melanocyte growth medium (Cascade M254-500). Human keratinocytes from neonatal foreskin samples were plated in two-well coverslips in C-154 media with KGS.

Immediately before incubation, a 10 μM SNARF-5F-AM (Molecular Probes, Eugene, OR) solution in melanocyte growth medium was prepared. Cells were incubated with the 10 μM dye solution for about 1 hour at 5% CO_2 and 37 °C. Before imaging, the dye containing medium was removed and the cells were rinsed once with melanocyte-growing media. A Zeiss LSM 510 Meta (Zeiss, Jena, Germany) was used to detect the pH-dependent spectral changes of the SNARF emission. The 488nm line of the Argon laser was used as the excitation line. A dichroic mirror reflecting wavelengths shorter than 635nm was used to split the fluorescence emission between two emission channels (Ch1 and Ch2). The Meta detector (used as Ch1) was set to detect light with wavelength longer than 623 nm. A band-pass filter centered at 563nm with a width of 55nm was placed in front of the PMT in Ch2. The pinholes in front of Ch1 and Ch2 were adjusted to give an optical slice of 0.8 μm with a ×63 oil objective. The gain and offset levels of the detectors were independently adjusted to ensure sensitivity in the pH range from 6 to 8. This was done by imaging a 5 μM solution of SNARF-5F in phosphate buffers at pH 5, 6, 7.4, and 8. The offset and gain levels of the detectors were then kept constant for all of the experiments.

Fluorescence intensity images collected in each channel were processed using Matlab (MathWorks, Natick, MA) after first eliminating artifacts due to a nonhomogeneous fluorescence intensity. Ch1 intensity was used to ascertain threshold levels of fluorescence for both channel intensity images. The spectral changes in the SNARF-5F emission were quantified by calculating the quantity *R*, defined below, pixel by pixel from the two images using the formula:

$$R\frac{I_{ch1} - I_{ch}}{I_{ch1} + I_{ch}}$$

where Ich1 and Ich2 are the intensities in Ch1 and Ch2, respectively. region of interests (ROIs) corresponding to cell bodies or dendrites were selected on the normalized ratio image using Image J software, and the average *R* values and SD are calculated for each ROI.

The values of *R* were converted to pH by performing an in-cell calibration in human keratinocytes. A pH 7.8 buffer with 13.5 μM nigericin (Sigma Aldrich) as the permeabilizing agent was added to one of the two wells, and keratinocytes were imaged every 10 seconds for about 20 minutes (we determined that about 10 minutes are needed for the intracellular pH spectra to equilibrate with the extracellular buffer). The same procedure was repeated on the second well of the cover slip using a 6.5 pH buffer with 13.5 μM nigericin. A linear dependence was assumed between *R* and pH. This assumption is based on the observed linear dependence of *R* on pH in solution (data not shown) over a pH range from 6 to 8.

Organotypic cell cultures

Primary cultures of human keratinocytes and melanocytes were established from neonatal foreskins of designated pigment types. Human keratinocytes and melanocytes were pipetted into polyethylene-coated transwells containing CnT-07 medium (Progenitor Cell Targeted culture medium with 0.07mM Ca^{++}; CELLnTEC Advanced Cell Systems, Bern, Switzerland) at 6:1 ratio, and incubated at 37 °C and 5% CO_2 for 72 hours. Cultures were then switched to CnT-02 medium (differentiation medium containing 1.2mM Ca^{++}) and exposed to air–liquid interface after 16 hours by removing most of the medium from transwells. They were then maintained at 37 °C with frequent media changes and harvested on day 10.

Statistical analyses

Two groups were compared with a Student's *t*-test. Nonparametric Mann–Whitney statistical analyses were performed to compare percentage of ratios between different groups of treatments. Statistical analyses were performed using Prism 3 (GraphPad software, San Diego, CA).

Supplementary Material

Refer to Web version on PubMed Central for supplementary material.

Abbreviations

CD
: corneodesmosome

CE
: cornified envelope

DSG-1
: desmoglein-1

GL
: gluconolactone

LB
: lamellar body

LBA
: lactobionic acid

SC
: stratum corneum

SG
: stratum granulosum

SP
: serine protease

TEWL
: transepidermal water loss

References

Bassnett S, Reinisch L, Beebe DC. Intracellular pH measurement using single excitation-dual emission fluorescence ratios. Am J Physiol 1990;258:C171–8. [PubMed: 2301564]

Behne MJ, Meyer JW, Hanson KM, Barry NP, Murata S, Crumrine D, et al. NHE1 regulates the stratum corneum permeability barrier homeostasis. Microenvironment acidification assessed with fluorescence lifetime imaging. J Biol Chem 2002;277:47399–406. [PubMed: 12221084]

Berardesca E, Distante F, Vignoli GP, Oresajo C, Green B. Alpha hydroxyacids modulate stratum corneum barrier function. Br J Dermatol 1997;137:934–8. [PubMed: 9470910]

Berardesca E, Pirot F, Singh M, Maibach H. Differences in stratum corneum pH gradient when comparing white Caucasian and black African-American skin. Br J Dermatol 1998;139:855–7. [PubMed: 9892954]

Bhatnagar V, Anjaiah S, Puri N, Darshanam BN, Ramaiah A. pH of melanosomes of B 16 murine melanoma is acidic: its physiological importance in the regulation of melanin biosynthesis. Arch Biochem Biophys 1993;307:183–92. [PubMed: 8239655]

Brattsand M, Egelrud T. Purification, molecular cloning, and expression of a human stratum corneum trypsin-like serine protease with possible function in desquamation. J Biol Chem 1999;274:30033–40. [PubMed: 10514489]

Brattsand M, Stefansson K, Lundh C, Haasum Y, Egelrud T. A proteolytic cascade of kallikreins in the stratum corneum. J Invest Dermatol 2005;124:198–203. [PubMed: 15654974]

Caubet C, Jonca N, Brattsand M, Guerrin M, Bernard D, Schmidt R, et al. Degradation of corneodesmosome proteins by two serine proteases of the kallikrein family, SCTE/KLK5/hK5 and SCCE/KLK7/hK7. J Invest Dermatol 2004;122:1235–44. [PubMed: 15140227]

Chen N, Seiberg M, Lin CB. Cathepsin L2 levels inversely correlate with skin color. J Invest Dermatol 2006;126:2345–7. [PubMed: 16728970]

Cork MJ, Robinson DA, Vasilopoulos Y, Ferguson A, Moustafa M, MacGowan A, et al. New perspectives on epidermal barrier dysfunction in atopic dermatitis: gene–environment interactions. J Allergy Clin Immunol 2006;118:3–21. [PubMed: 16815133]quiz 22–23

Demerjian M, Man MQ, Choi EH, Brown BE, Crumrine D, Chang S, et al. Tropical treatment with thiazolidinedlones, activators of peroxisome proliferatoractivated receptor-gamma, normalizes epidermal homeostasis in a murine hyperproliferative disease model. Exp Dermatol 2006;15:154–60. [PubMed: 16480422]

Denda M, Sato J, Masuda Y, Tsuchiya T, Koyama J, Kuramoto M, et al. Exposure to a dry environment enhances epidermal permeability barrier function. J Invest Dermatol 1998;111:858–63. [PubMed: 9804350]

Dreher F, Arens A, Hostynek JJ, Mudumba S, Ademola J, Maibach HI. Colorimetric method for quantifying human stratum corneum removed by adhesive-tape stripping. Acta Derm Venereol 1998;78:186–9. [PubMed: 9602223]

Egberts F, Heinrich M, Jensen JM, Winoto-Morbach S, Pfeiffer S, Wickel M, et al. Cathepsin D is involved in the regulation of transglutaminase 1 and epidermal differentiation. J Cell Sci 2004;117:2295–307. [PubMed: 15126630]

Ekholm IE, Brattsand M, Egelrud T. Stratum corneum tryptic enzyme in normal epidermis: a missing link in the desquamation process? J Invest Dermatol 2000;114:56–63. [PubMed: 10620116]

Elias PM. Stratum corneum defensive functions: an integrated view. J Invest Dermatol 2005;125:183–200. [PubMed: 16098026]

Elias PM, Menon GK. Structural and lipid biochemical correlates of the epidermal permeability barrier. Adv Lipid Res 1991;24:1–26. [PubMed: 1763710]

Elias PM, Schmuth M, Uchida Y, Rice RH, Behne M, Crumrine D, et al. Basis for the permeability barrier abnormality in lamellar ichthyosis. Exp Dermatol 2002;11:248–56. [PubMed: 12102664]

Fitzpatrick TB. The validity and practicality of sun-reactive skin types I through VI. Arch Dermatol 1988;124:869–71. [PubMed: 3377516]

Fluhr JW, Elias PM. Stratum corneum pH: formation and function of the “acid mantle”. Exog Dermatol 2002;1:163–75.

Fluhr JW, Kao J, Jain M, Ahn SK, Feingold KR, Elias PM. Generation of free fatty acids from phospholipids regulates stratum corneum acidification and integrity. J Invest Dermatol 2001;117:44–51. [PubMed: 11442748]

Fluhr JW, Mao-Qiang M, Brown BE, Hachem JP, Moskowitz DG, Demerjian M, et al. Functional consequences of a neutral pH in neonatal rat stratum corneum. J Invest Dermatol 2004;123:140–51. [PubMed: 15191554]

Hachem JP, Crumrine D, Fluhr J, Brown BE, Feingold KR, Elias PM. pH directly regulates epidermal permeability barrier homeostasis, and stratum corneum integrity/cohesion. J Invest Dermatol 2003;121:345–53. [PubMed: 12880427]

Hachem JP, Houben E, Crumrine D, Man MQ, Schurer N, Roelandt T, et al. Serine protease signaling of epidermal permeability barrier homeostasis. J Invest Dermatol 2006;126:2074–86. [PubMed: 16691196]

Hachem JP, Man MQ, Crumrine D, Uchida Y, Brown BE, Rogiers V, et al. Sustained serine proteases activity by prolonged increase in pH leads to degradation of lipid processing enzymes and profound alterations of barrier function and stratum corneum integrity. J Invest Dermatol 2005;125:510–20. [PubMed: 16117792]

Horikoshi T, Igarashi S, Uchiwa H, Brysk H, Brysk MM. Role of endogenous cathepsin D-like and chymotrypsin-like proteolysis in human epidermal desquamation. Br J Dermatol 1999;141:453–9. [PubMed: 10583048]

Hunter RC, Beveridge TJ. Application of a pH-sensitive fluoroprobe (C-SNARF-4) for pH microenvironment analysis in *Pseudomonas aeruginosa* biofilms. Appl Environ Microbiol 2005;71:2501–10. [PubMed: 15870340]

Jimbow K, Quevedo WC Jr, Fitzpatrick TB, Szabo G. Some aspects of melanin biology: 1950–1975. J Invest Dermatol 1976;67:72–89. [PubMed: 819593]

Korting HC, Hubner K, Greiner K, Hamm G, Braun-Falco O. Differences in the skin surface pH and bacterial microflora due to the long-term application of synthetic detergent preparations of pH 5.5 and pH 7.0. Results of a crossover trial in healthy volunteers. Acta Derm Venereol 1990;70:429–31. [PubMed: 1980979]

Mackintosh JA. The antimicrobial properties of melanocytes, melanosomes and melanin and the evolution of black skin. J Theor Biol 2001;211:101–13. [PubMed: 11419954]

Marchionini A, Hausknecht W. Sauremantel der haut and bakterienabwehr. Klin Wochenschr 1938;17:663–6.

Mauro T, Holleran WM, Grayson S, Gao WN, Man MQ, Kriehuber E, et al. Barrier recovery is impeded at neutral pH, independent of ionic effects: implications for extracellular lipid processing. Arch Dermatol Res 1998;290:215–22. [PubMed: 9617442]

McEvoy B, Beleza S, Shriver MD. The genetic architecture of normal variation in human pigmentation: an evolutionary perspective and model. Hum Mol Genet 2006;15(Spec2):R176–81. [PubMed: 16987881]

Nylander-Lundqvist E, Back O, Egelrud T. IL-1 beta activation in human epidermis. J Immunol 1996;157:1699–704. [PubMed: 8759758]

Pinnagoda J, Tupker RA, Agner T, Serup J. Guidelines for transepidermal water loss (TEWL) measurement. A report from the Standardization Group of the European Society of Contact Dermatitis. Contact Dermatitis 1990;22:164–78. [PubMed: 2335090]

Puri N, Gardner JM, Brilliant MH. Aberrant pH of melanosomes in pink-eyed dilution (p) mutant melanocytes. J Invest Dermatol 2000;115:607–13. [PubMed: 10998131]

Rawlings AV. Ethnic skin types: are there differences in skin structure and function? Int J Cosmet Sci 2006;28:79–93. [PubMed: 18492142]

Rawlings AV, Davies A, Carlomusto M, Pillai S, Zhang K, Kosturko R, et al. Effect of lactic acid isomers on keratinocyte ceramide synthesis, stratum corneum lipid levels and stratum corneum barrier function. Arch Dermatol Res 1996;288:383–90. [PubMed: 8818186]

Reed JT, Ghadially R, Elias PM. Skin type, but neither race nor gender, influence epidermal permeability barrier function. Arch Dermatol 1995;131:1134–8. [PubMed: 7574829]

Rogers J, Harding C, Mayo A, Banks J, Rawlings A. Stratum corneum lipids: the effect of ageing and the seasons. Arch Dermatol Res 1996;288:765–70. [PubMed: 8950457]

Schade H. Zur physikalischen chemie der hautoberflache. Arch Dermatol Syphilis 1928;154:690–716.

Szabo G, Gerald AB, Pathak MA, Fitzpatrick TB. Racial differences in the fate of melanosomes in human epidermis. Nature 1969;222:1081–2. [PubMed: 5787098]

Thong HY, Jee SH, Sun CC, Boissy RE. The patterns of melanosome distribution in keratinocytes of human skin as one determining factor of skin colour. Br J Dermatol 2003;149:498–505. [PubMed: 14510981]

Uchida Y, Holleran WM. Omega-*O*-acylceramide, a lipid essential for mammalian survival. J Dermatol Sci 2008;51:77–87. [PubMed: 18329855]

Whitaker JE, Haugland RP, Prendergast FG. Spectral and photophysical studies of benzo[c]xanthene dyes: dual emission pH sensors. Anal Biochem 1991;194:330–44. [PubMed: 1862936]

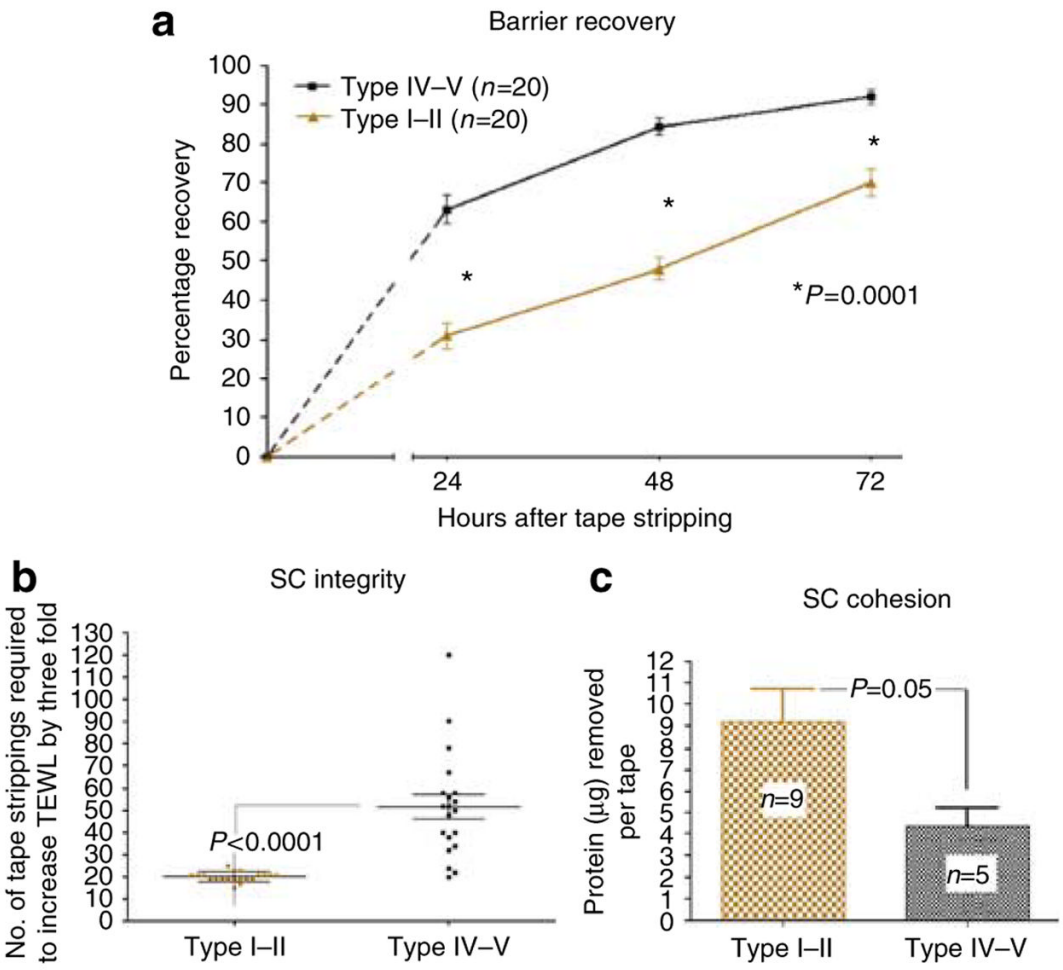

Figure 1. Type IV–V subjects show faster barrier recovery kinetics, and better SC integrity and cohesion

The volar forearms of pigment types I–II and IV–V subjects were tape-stripped until TEWL was increased threefold. TEWL was measured immediately, and 24, 48, and 72 hours, after acute barrier disruption. For calculation of the percentage change in TEWL, the following formula was used: (TEWL immediately after stripping−TEWL at the indicated time)/(TEWL immediately after stripping–baseline TEWL) × 100%. Baseline TEWL for the two populations was normal (≤ 10 gm^{-2} hour^{-1}). Type IV–V subjects (**a**) showed significantly faster epidermal barrier recovery at 24, 48, and 72 hours, (**b**) needed a significantly higher number of tape strippings to produce a comparable barrier disruption, and (**c**) had significantly less protein removed per tape stripping. Results shown represent means ± SEM.

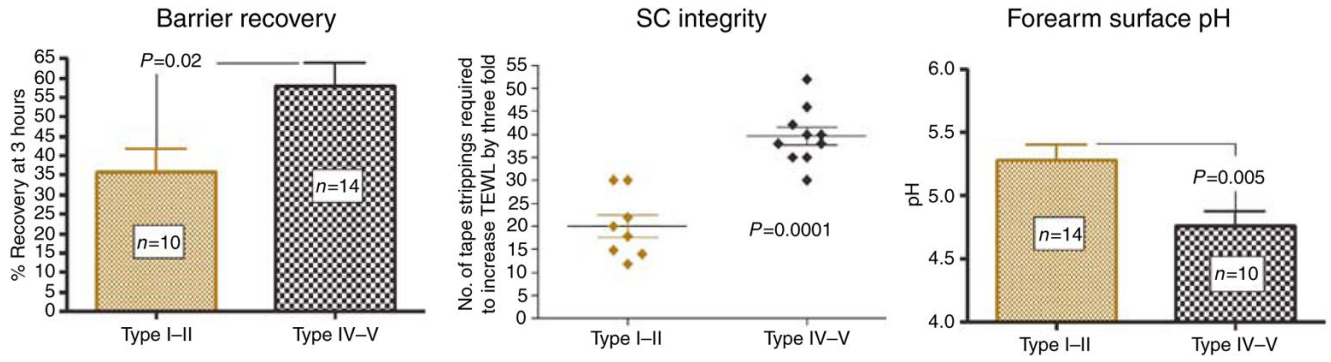

Figure 2. Epidermal functional differences among divergent pigment groups are independent of geographic location and occupation

Barrier recovery, epidermal integrity, and forearm surface pH were assessed in a cohort of subjects with type I–II and IV–V skin, living in the same geographic location (San Francisco, CA). None of the subjects were involved in nursing or related occupations. SC integrity was assessed as the number of D-squame tape strippings required to increase TEWL by threefold. TEWL was assessed immediately and 3 hours after barrier disruption and percentage of recovery was calculated as described previously. The baseline TEWL for the two pigment groups was $\leq 10\ gm^{-2}\ hour^{-1}$. Surface pH of the volar forearm was measured using a flat glass electrode.

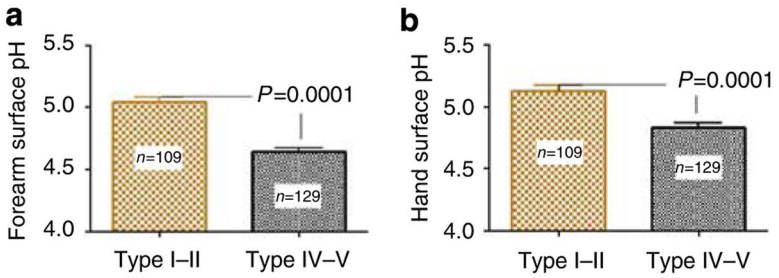

Figure 3. Type IV–V subjects have more acidic SC surface pH

Surface pH of the (**a**) volar forearm and (**b**) dorsum of the hand was measured in two age-matched groups of German (n = 110, 72 females, age 29 ± 6.6) and Sri Lankan (n = 129, 117 females, age 25 ± 2.1) nurses with type I–II and IV–V skin using a flat glass electrode. Type IV–V subjects had significantly more acidic surface pH. Results shown represent means ± SEM.

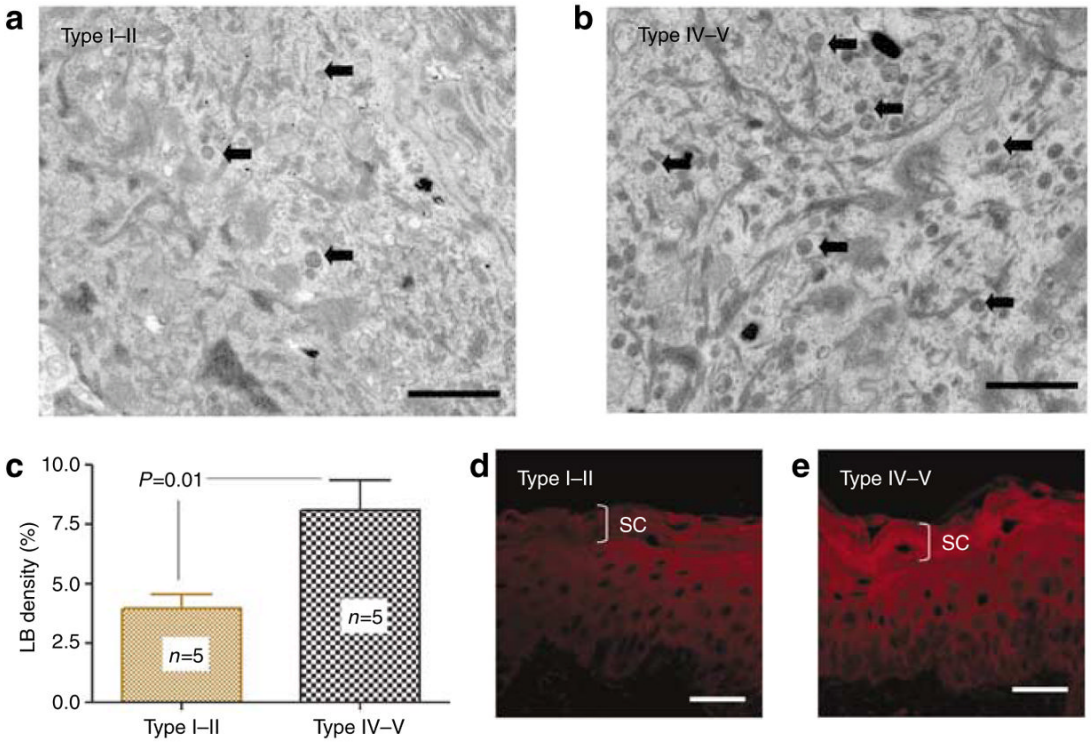

Figure 4. Darkly pigmented subjects have more lamellar bodies (LBs) and barrier lipids

(**a**–**c**) The darkly pigmented skin has higher LB density as illustrated by random electron micrographs (**a**, **b**: osmium tetroxide postfixation, Bar = 1 μm), and assessed by quantitative electron microscopy. (**c**) The granular layer immediately below the SC–SG junction is shown. Block arrows point to LBs. Results shown represent means ± SEM. (**d**, **e**) This finding correlated with increased SC lipid content as shown by Nile Red fluorescence in frozen sections. Bar = 40 μm.

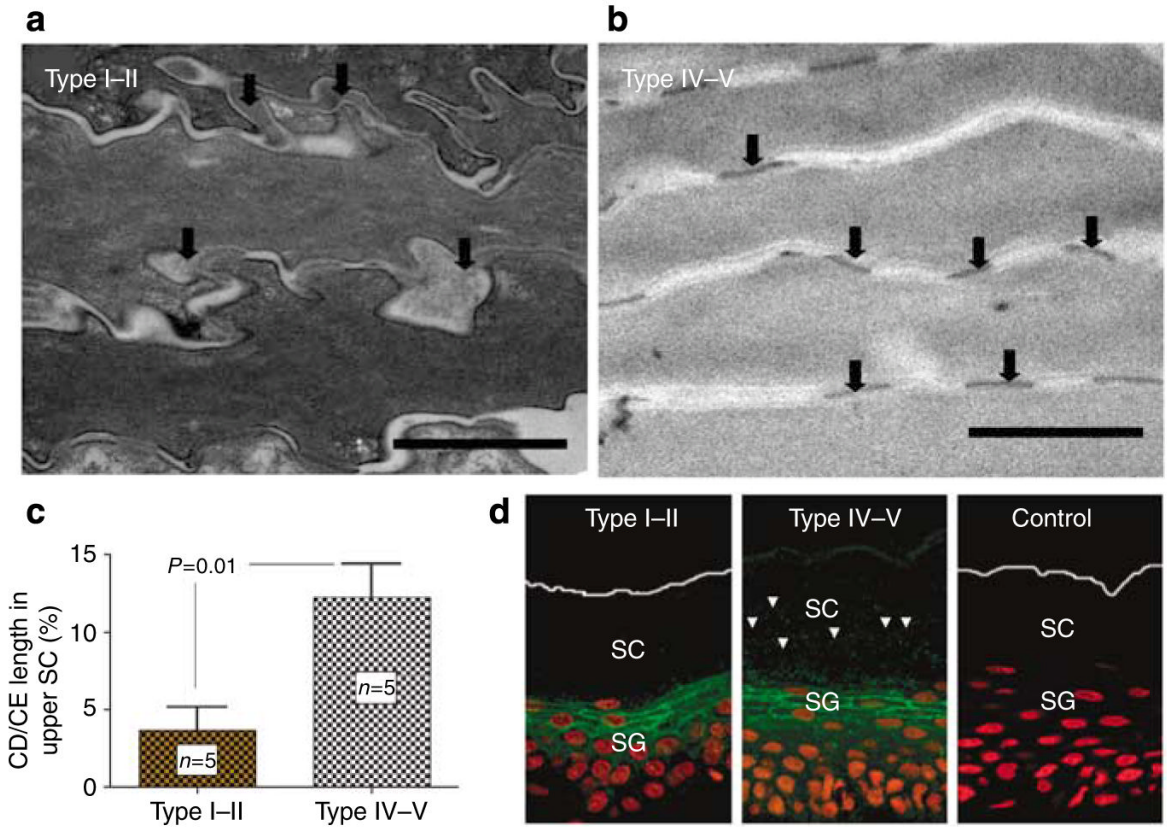

Figure 5. Persistence of corneodesmosomes (CDs) in the upper SC of darkly pigmented skin is paralleled by decreased SP dependent degradation of Desmosglein-1 (DSG-1)

(**a–c**) Darkly pigmented subjects have significant retention of CDs in the upper SC as shown by quantitative electron microscopy. In contrast, the CDs in the upper SC of lightly pigmented skin appeared to be degraded osmium tetroxide postfixation (Bar = 1 μm). CD and cornified envelope (CE) length was measured in sequential electron micrographs by planimetry, and CD length was expressed as a percentage of CE length. Results shown represent means ± SEM. (**d**) Immunofluorescence staining shows parallel retention of DSG-1 in the SC of darkly pigmented skin despite comparable DSG-1 expression at stratum granulosum level. Bar = 40 μm.

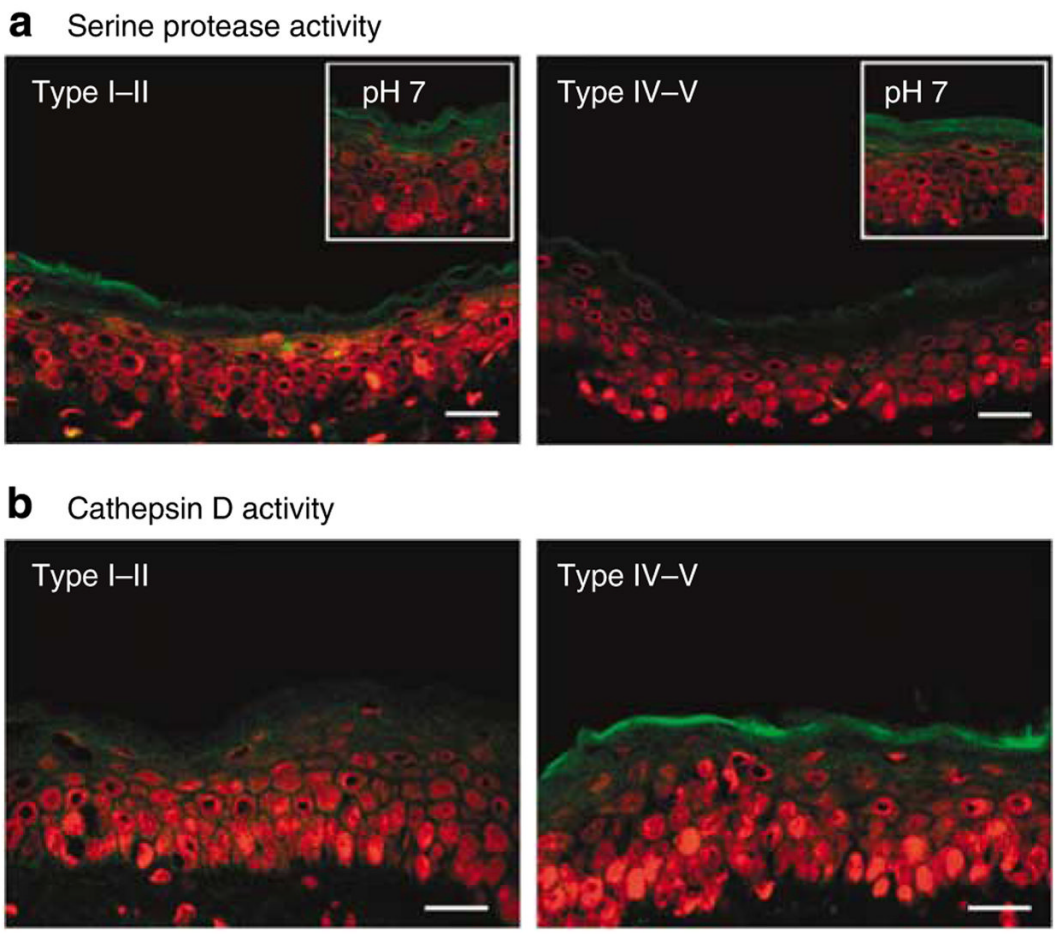

Figure 6. Serine protease inactivation by more acidic surface pH accounts for persistence of corneodesmosomes in the upper SC in darkly pigmented subjects, but increased acidic-dependent protease activity maintains normal SC thickness

(**a**) Type IV–V darkly pigmented subjects with more acidic surface pH have lower SP activity under basal conditions as shown by *in situ* zymography. Inset: *in vitro* neutralization of sections with 4-(2-hydroxyethyl)- 1-piperazineethanesulfonic acid buffer (pH 7) induced SP activity to comparable levels, showing that differences in activity are pH driven, rather than being attributable to different levels of enzyme protein. Bar = 40 μm. (**b**) *In situ* zymography of frozen sections shows increased activity of cathepsin D, an aspartate protease with acidic pH optimum, in darkly pigmented skin. Bar = 40 μm.

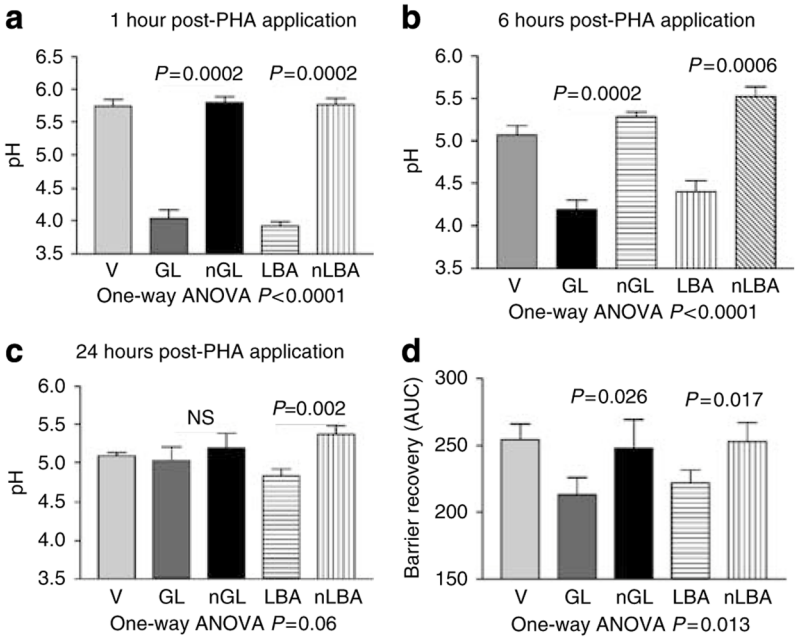

Figure 7. Single applications of either polyhydroxyl acids decrease SC pH and accelerate barrier recovery in lightly pigmented subjects

(**a–c**) Lactobionic acid (LBA, 5% in propylene glycol/ethanol: 70/30), gluconolactone (GL), neutralized LBA, neutralized GL, or vehicle (V) was applied on the forearm skin of human volunteers (n = 16). Although basal values were identical on all test sites before application (not shown), significant decreases in surface pH were observed at 1, 6, and 24 hours following single application of either LBA or GL acids compared with the vehicle. (**d**) TEWL was measured before and at 0, 3, 24, and 48 hours following acute barrier disruption by repeated cellophane tape stripping on the forearms of type I–II subjects. Acidification of SC pH by PHA (LBA or GL, n = 16) significantly improved barrier recovery in comparison with vehicle (neutralized LBA/neutralized GL)-treated skin sites.

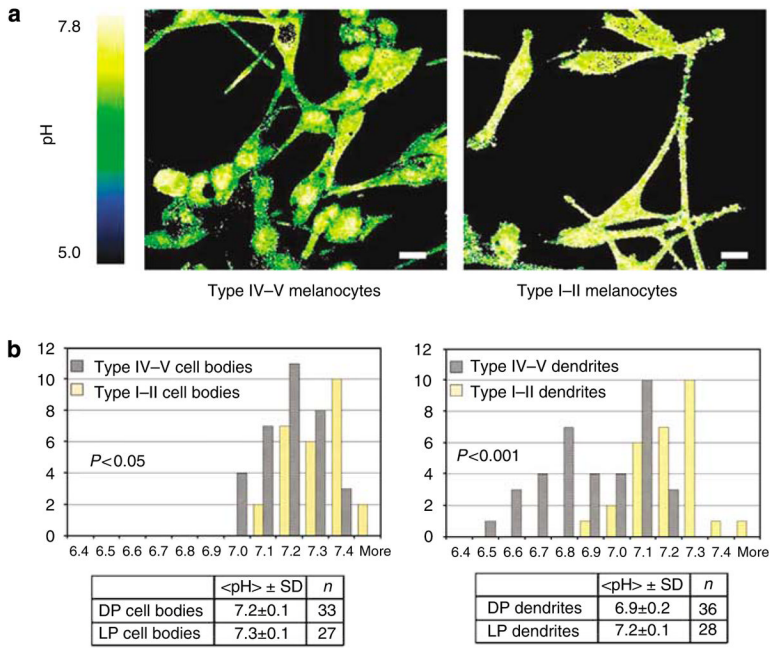

	<pH> ± SD	n
DP cell bodies	7.2±0.1	33
LP cell bodies	7.3±0.1	27

	<pH> ± SD	n
DP dendrites	6.9±0.2	36
LP dendrites	7.2±0.1	28

Figure 8. Melanocytic dendrites are significantly more acidic in the darkly pigmented subjects

(**a**) Two-channel confocal imaging of human melanocytes stained with the pH-sensitive probe SNARF-5F shows that dendrites, but not the cell bodies, of darkly pigmented melanocytes (taken from type IV–V skin) are significantly more acidic, in comparison with those of lightly pigmented melanocyte (taken from type I–II skin). The color bar on the left of the image indicates the pH range corresponding to the *R* color-coding used in the figures, with green indicating more acidic pH, while yellow denotes more neutral pH. Bar = 15 μm. (**b**) The spectral changes in the SNARF-5F emission were used to quantify R, and *R* values were used to derive pH (see under Materials and methods). Both the cytosol and dendrites were significantly more acidic in the darkly pigmented melanocytes.

Table 1

Demographic characteristics of the study subjects with divergent pigment types from three geographically disparate locations

Geographic location	Temp/RH	Pigment type	n	Females	Age ± SD
Osnabruck, Germany	15–25 °C	I–II	110	72	29.3±6.6
	55–80%				
Colombo, Sri Lanka	27–30 °C	IV–V	129	117	25.0±2.1
	60–80%				
San Francisco, CA	23–28 °C	I–II	14	10	32.4±4.1
	30–45%	IV–V	10	6	34.1±3.2